

UC San Diego

UC San Diego Previously Published Works

Title

Impacts of H<sub>2</sub>O<sub>2</sub>, SARM1 inhibition, and high NAM concentrations on Huntington's disease laser-induced degeneration

Permalink

<https://escholarship.org/uc/item/2kr0k35c>

Authors

Barber, Sophia

Gomez-Godinez, Veronica

Young, Joy

et al.

Publication Date

2024-01-07


DOI

10.1002/jbio.202300370

Peer reviewed

## RESEARCH ARTICLE

# Impacts of H<sub>2</sub>O<sub>2</sub>, SARM1 inhibition, and high NAM concentrations on Huntington's disease laser-induced degeneration

Sophia Barber<sup>1,2</sup> | Veronica Gomez-Godinez<sup>1</sup> | Joy Young<sup>1</sup> | Abigail Wei<sup>1</sup> | Sarah Chen<sup>1</sup> | Anna Snissarenko<sup>2</sup> | Sze Sze Chan<sup>2</sup> | Chengbiao Wu<sup>1,2</sup> | Linda Shi<sup>1</sup> 

<sup>1</sup>Institute of Engineering in Medicine, University of California San Diego, La Jolla, California, USA

<sup>2</sup>Department of Neurosciences, University of California San Diego, La Jolla, California, USA

## Correspondence

Veronica Gomez-Godinez and Linda Shi, Institute of Engineering in Medicine, University of California San Diego, La Jolla, CA 92093, USA.  
Email: [vgomez-godinez@ucsd.edu](mailto:vgomez-godinez@ucsd.edu) and [zshi@ucsd.edu](mailto:zshi@ucsd.edu)

## Funding information

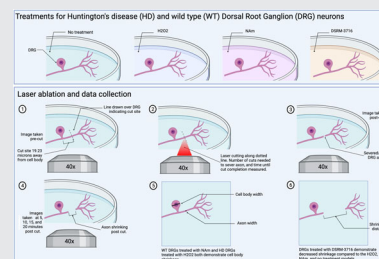
Beckman Laser Inc

## Abstract

Axonal degeneration is a key component of neurodegenerative diseases such as Huntington's disease (HD), Alzheimer's disease, and amyotrophic lateral sclerosis. Nicotinamide, an NAD<sup>+</sup> precursor, has long since been implicated in axonal protection and reduction of degeneration. However, studies on nicotinamide (NAM) supplementation in humans indicate that NAM has no protective effect. Sterile alpha and toll/interleukin receptor motif-containing protein 1 (SARM1) regulates several cell responses to axonal damage and has been implicated in promoting neuronal degeneration. SARM1 inhibition seems to result in protection from neuronal degeneration while hydrogen peroxide has been implicated in oxidative stress and axonal degeneration. The effects of laser-induced axonal damage in wild-type and HD dorsal root ganglion cells treated with NAM, hydrogen peroxide (H<sub>2</sub>O<sub>2</sub>), and SARM1 inhibitor DSRM-3716 were investigated and the cell body width, axon width, axonal strength, and axon shrinkage post laser-induced injury were measured.

## KEYWORDS

axonal damage, cell morphology, dorsal root ganglion cells, Huntington's disease, laser cutting, neurons



Sophia Barber and Veronica Gomez-Godinez contributed equally to this work.

The statements, opinions, and data contained in all publications are solely those of the individual author(s) and contributor(s) and not of Journal of Biophotonics and/or the editor(s). Journal of Biophotonics and/or the editor(s) disclaim responsibility for any injury to people or property resulting from any ideas, methods, instructions, or products referred to in the content.

This is an open access article under the terms of the [Creative Commons Attribution-NonCommercial-NoDerivs](https://creativecommons.org/licenses/by-nc-nd/4.0/) License, which permits use and distribution in any medium, provided the original work is properly cited, the use is non-commercial and no modifications or adaptations are made.

© 2024 The Authors. *Journal of Biophotonics* published by Wiley-VCH GmbH.

## 1 | INTRODUCTION

Huntington's disease (HD) is a progressive, autosomal dominant, and fatal neurodegenerative disorder characterized by cognitive, psychiatric, and motor decline [1]. Huntington's disease onset occurs between the ages of 35 and 44 and results from an expanded CAG repeat (>36) in exon 1 of the huntingtin (HTT) gene which encodes for an abnormally long polyglutamine repeat (polyQ) [2–6]. The accumulation of mutant huntingtin (mHTT) within neurons leads to general shrinkage of the brain and preferential degeneration of the striatum, especially in the medium spiny neurons (MSNs) and parvalbumin-expressing interneurons within the striatum [7–11]. In addition, mHTT results in regionally specific heterogeneous thinning of the cortical ribbon [12]. MSNs and cortical projection neurons seem to be particularly affected by mHTT accumulation due to the length and prominence of their axons [13]. HD patients generally survive 15–20 years after manifestation of definitive motor symptoms suggestive of HD with no other explanation [5, 14].

Clinical motor presentations include involuntary movement in early HD disease and impaired voluntary movement in advanced HD disease [5, 15]. Chorea, defined as short-lived, excessive, involuntary movements, is one of the most striking motor features of HD disease [5, 15]. Cognitive deficits in HD can occur years before disease onset. These early deficits are found in visual attention, psychomotor speed, and visuomotor and spatial integration, although are often not severe enough for patients to self-identify [16]. Advanced stages of HD cognitive decline are characterized by subcortical and frontal dementia [16]. While not related to disease onset, of psychiatric problems in HD, depression and anxiety are the most common, with depression affecting ~40% of patients [17, 18]. Apathy, characterized by a general loss of interest, passivity, and difficulty initiating activities, is directly linked to the disease stage HD, worsens over time, and is resistant to medication [19]. Other psychiatric symptoms include obsessive and compulsive thoughts and behaviors, irritability, and even psychosis which occurs more rarely and in more advanced stages of HD [17, 20, 21]. Additionally, according to a study of 4171 HD patients, 10% of patients had attempted suicide and 17.5% indicated that they had suicidal thoughts [22].

Despite HD classification as a central nervous system (CNS) disease, recent studies have shown systemwide impacts of mHTT on peripheral tissues as well [23]. Thus, it is imperative that the effects of mHTT accumulation on peripheral neurons also be studied. Dorsal root ganglions (DRGs), peripheral neurons which are responsible for the transmission of pain and proprioception to the CNS, provide a unique avenue to study the impacts of Huntington's disease on the peripheral nervous system [24]. DRGs are

pseudo-unipolar with a single axon that branches into long distal and proximal processes [25]. The increased vulnerability of longer and more prominent axons to accumulation of mHTT as seen in MSN and cortical projection neurons makes the pseudo-unipolar structure of DRGs particularly useful in studying and assessing the HD impacts in axons of the peripheral nervous system (PNS) neurons.

We used a robotic laser microscope system (RoboLase) to investigate the impacts of mHTT on the axonal resistance to damage in DRGs. The RoboLase system allowed for high precision in axonal cutting, creating just enough damage to sever the axon without destroying the cell. The effects of oxidative stress, high concentrations of nicotinamide, and SARM1 inhibition on axonal strength and resistance to damage in HD neurons were studied to provide insight into the impacts of mHTT accumulation on treatment susceptibility to axonal stressors and axonal protective compounds. Hydrogen peroxide ( $H_2O_2$ ) creates oxidative stress in neurons and results in axonal degeneration [26, 27]. Nicotinamide (NAM) has been demonstrated to have axonal protective effects, and neurons treated with nicotinamide have shown a reduction in degeneration [28]. However, recent studies on the effects of NAM supplementation in humans have demonstrated no effect [29]. Studies on the effects of high concentrations of NAM on cancer cells have shown a cytotoxic effect [30]. Recent studies have found also that SARM1 (sterile alpha and toll/interleukin receptor [TIR] motif-containing protein 1) plays an important role in promoting neuronal degeneration. Studies in SARM1 inhibition found that inhibition results in protection from neuronal degeneration [31]. We hope to elucidate the distinct effects of  $H_2O_2$ , nicotinamide, and SARM1 inhibition on wild-type and Huntington's disease DRGs and determine if there are differences in their effects between the three models.

## 2 | MATERIALS AND METHODS

### 2.1 | RoboLase set up

The robotic laser microscope system III (RoboLase III) was used to cut the axons of DRGs. The RoboLase III system employed a Mai Tai femtosecond laser. The beam was coupled to Zeiss inverted microscope via a series of highly reflective coated mirrors. A wavelength of 790 nm, a pulse energy of 4 nJ, and an average power of 395 mW was set before a 40x objective targeting the desired axon. Several different powers were tested to determine a power which would cut cleanly through the axon while inflicting the least damage possible. The ablation was applied precisely along a drawn line and images were captured using a QuantEM camera. Figure 1 demonstrates the RoboLase III system graphically and was created with [BioRender.com](https://www.biorender.com).

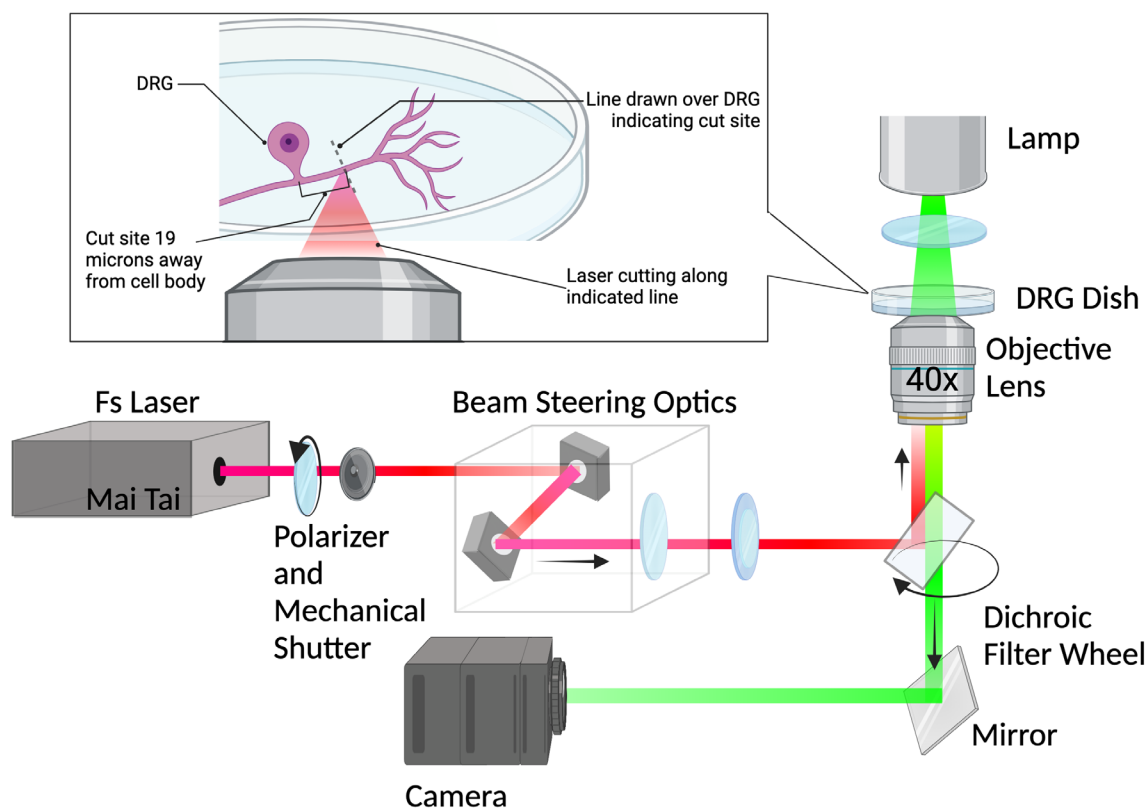


FIGURE 1 Graphical diagram of the RoboLase III system used to perform DRG experiments. Created with BioRender.com.

## 2.2 | Animals

All experiments involving the use of animals have been approved by the Institutional Animal Care and Use Committee of University of California San Diego. All experimental procedures were performed in accordance with relevant guidelines and regulations established by NIH Guide for the Care and Use of Laboratory Animals. All animals were bred and maintained following standard procedures. Wild-type mice and mice from a bacterial artificial chromosome (BAC)-mediated transgenic mouse model (BACHD) were bred to create wild-type and transgenic embryos and pups [32]. E18 through P0 pups were used to collect and culture Dorsal Root Ganglions (DRGs).

## 2.3 | Genotyping

Established protocols were followed to perform genotyping procedures [32]. The BACHD model expressed the full-length human mutant huntingtin (fl-mhtt) with 97 glutamine repeats on the BAC [32]. 1 cm tail pieces were removed from pups and were digested in 50 mM NaOH for 30 min at 95°C. Once digested, the NaOH was quenched using 0.5 M Tris, and the tubes were centrifuged for 10 min at 13 k rpm to generate the tail supernatant. The PCR was performed with BACHD primers in line with the BACHD

PCR settings outlined in Gray et al. [32]. The primers used were Htt5: 5' GAG CCA TGA TTG TGC TAT CG 3' and Htt3: 5'AGC TAC GCT GCT CAC AGA AA 3'. Once the PCR was completed, the PCR products were run on a 2% agarose gel for 20 min under 120 V. The presence of a 400 bp was used to determine the transgenic genotype while the wild-type samples did not yield this 400 bp PCR product.

## 2.4 | Chemicals, reagents, and media

The chemicals and reagents purchased for the primary neuron culture are 10× Hank's Balanced Salt Solution (HBSS) (Gibco, Cat#14185-052), Pen Strep (100×) (Gibco, Cat#15140-122), Glutamax (100×) (Gibco, Cat#35050-061), 2.5% Trypsin (10×), no phenol red (Gibco, Catalog #: 15090046), 10× DNase I (Roche, # 10104159001, 100 mg package, dissolved in 10 mL 1× HBSS to final 10 mg/mL and filter to sterilize), Poly-D-Lysine (ThermoFisher, Cat#A3890401), Neurobasal Medium (–Glutamine) (1×) (Gibco, Cat#10888-022) or 21103-49, B27 Supplements (50×) (Gibco, Cat#17504-044), and AraC (crystalline, ≥90% (HPLC)) (Sigma-Aldrich, CAS#147-94-4). The chemicals and reagents purchased for nicotinamide treatments were Sigma-Aldrich, #50-188-2894. The chemicals and reagents purchased for H<sub>2</sub>O<sub>2</sub> treatments were Sigma-Aldrich, CAS# 7722-84-1.

## 2.5 | Primary neuron culture

DRGs were dissected from HD transgenic and WT mouse pups following established protocols [33, 34]. DRGs were removed from the dorsal column and placed in HBSS with 1% pen/strep. Neurons were dissociated and resuspended in plating media with 1% GlutaMAX, 1% B27, 10% FBS, and 100 ng/mL NGF. Neurons were placed on 35 mm glass-bottom imaging dishes precoated with Poly-D-Lysine and were then placed in the incubator for 24 h. The next day, the media was replaced with anti-mitotic plating media, consisting of 1% GlutaMAX, 1% B27, 100 ng/mL NGF, and 5  $\mu$ M AraC to suppress the Schwann cells. 48 h later they were transitioned to normal plating media, consisting only of 1% GlutaMAX, 1% B27, and 100 ng/mL NGF. Axonal cutting, treatment, and imaging using the RoboLase III system took place on DIV 3 and DIV 4.

## 2.6 | Untreated neurons

Untreated neurons were used to determine treatment effectiveness. Untreated neurons were stored in a 37°C, 5% CO<sub>2</sub> humidified incubator with treated neurons before imaging.

## 2.7 | Neurons treated with 100 $\mu$ M H<sub>2</sub>O<sub>2</sub>

To test the degenerative effect of H<sub>2</sub>O<sub>2</sub>, established protocols by Fang et al. were followed [27]. WT and BACHD DRGs in the H<sub>2</sub>O<sub>2</sub> treatment group were treated with 100  $\mu$ M H<sub>2</sub>O<sub>2</sub> in plating media and placed in a 5% CO<sub>2</sub> humidified incubator for 1 h before imaging.

## 2.8 | Neurons treated with 24.5 mM nicotinamide

To test the protective effect of Nicotinamide, established protocols by Wang et al. were followed [35]. The current range of safe concentrations of nicotinamide is 5–25 mM. WT and BACHD DRGs in the Nicotinamide treatment group were treated with 24.5 mM Nicotinamide in plating media and placed in a 5% CO<sub>2</sub> humidified incubator for 24 h before imaging.

## 2.9 | Neurons treated with 30 $\mu$ M SARM1 inhibitor

To test the protective effect of SARM1 inhibition, established protocols by Hughes et al. were followed [36]. WT

and BACHD DRGs in the SARM1 inhibitor treatment group were treated with 30  $\mu$ M SARM1 inhibitor (DSRM-3716) in plating media and placed in a 5% CO<sub>2</sub> humidified incubator for 10 min before imaging.

## 2.10 | Data collection

Images were taken before the DRGs were cut with RoboLase III (pre-cut), immediately after they were cut (post-cut), and at 5, 10, 15, and 20 min post-cut. Axons were cut 19.23 microns away from the cell body. Cell bodies were identified by their round shape and the halo of light around them. Fiji was used to analyze collected images for variation in cell body widths, axonal widths, and axonal shrinkage and segmentation post-cut.

## 2.11 | Statistical analysis

Statistical significance analysis was performed using Prism. Significances were calculated using One Way ANOVA or Two Way ANOVA. The specific methods are indicated in their respective figures. The mean  $\pm$  SD values are indicated for each bar graph. Ns: non significance; \* $p$  < 0.05; \*\* $p$  < 0.01; \*\*\* $p$  < 0.001; \*\*\*\* $p$  < 0.0001.

# 3 | RESULTS

## 3.1 | Cell body and axonal width variation

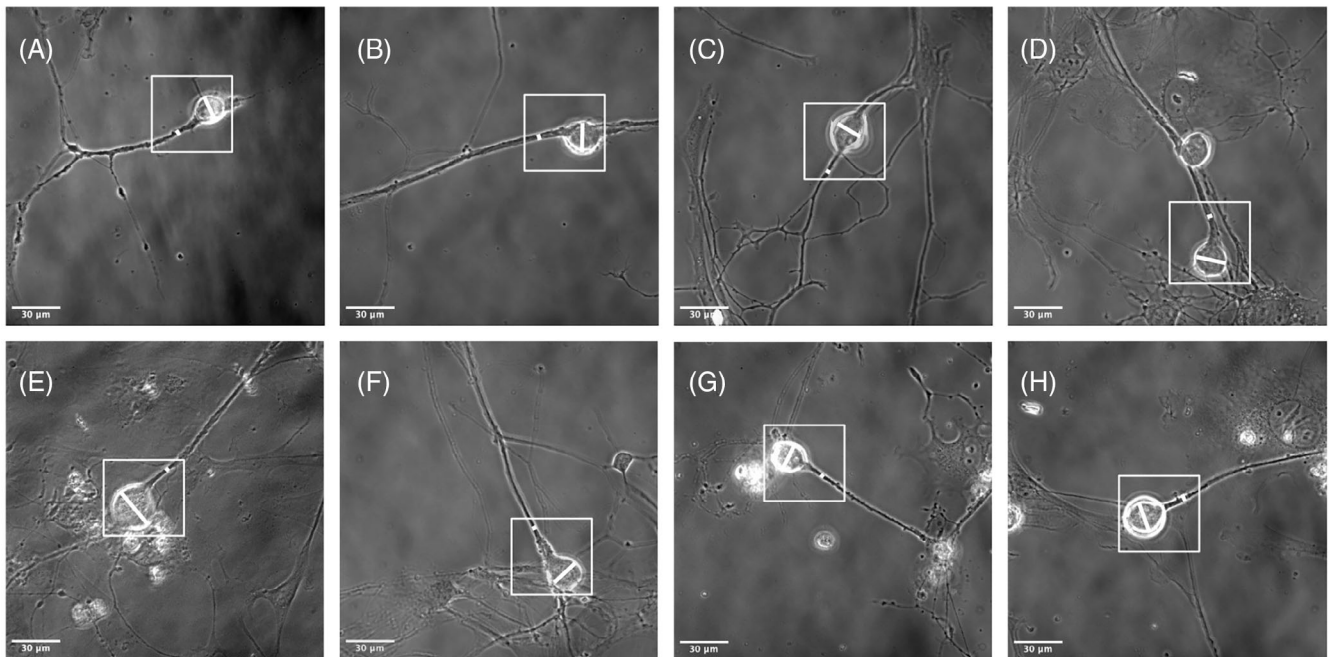
Innate and treatment-induced morphology changes were the first metrics we used to study the impacts of Huntington's disease on PNS neurons. To determine this, we measured the cell body width and axonal width of each DRGs from the studied models: Wild-type (WT) control, Huntington's disease (HD) control, WT treated with H<sub>2</sub>O<sub>2</sub>, HD treated with H<sub>2</sub>O<sub>2</sub>, WT treated with NAM, HD treated with NAM, WT treated with DSRM-3716, and HD treated with DSRM-3716. Figure 2A–H are representative images of a WT Control DRG, an HD Control DRG, a WT H<sub>2</sub>O<sub>2</sub> DRG, an HD H<sub>2</sub>O<sub>2</sub> DRG, a WT NAM DRG, an HD NAM DRG, a WT DSRM-3716 DRG, and an HD DSRM-3716 DRG, respectively, before being sliced by the RoboLase laser. Within the white box is the DRG cell body and the part of the axon that was measured. The white lines going across the cell body and across the axon represent the distinctive cell body width and axonal width measurements.

Figure 2I graphically compares the cell body widths and axonal widths of WT and HD models, and their



respective treatment groups. We found a significant difference between WT Control and WT NAM cell body widths such that WT DRGs treated with NAM on average have smaller cell body widths. While NAM does seem to

have a shrinkage effect on WT DRG cell bodies, NAM does not have a similar effect on HD DRGs. No difference was found in the widths of the cell bodies of HD Control DRGs and HD DRGs treated with NAM. HD DRGs seem



(I) Cell body and axon widths

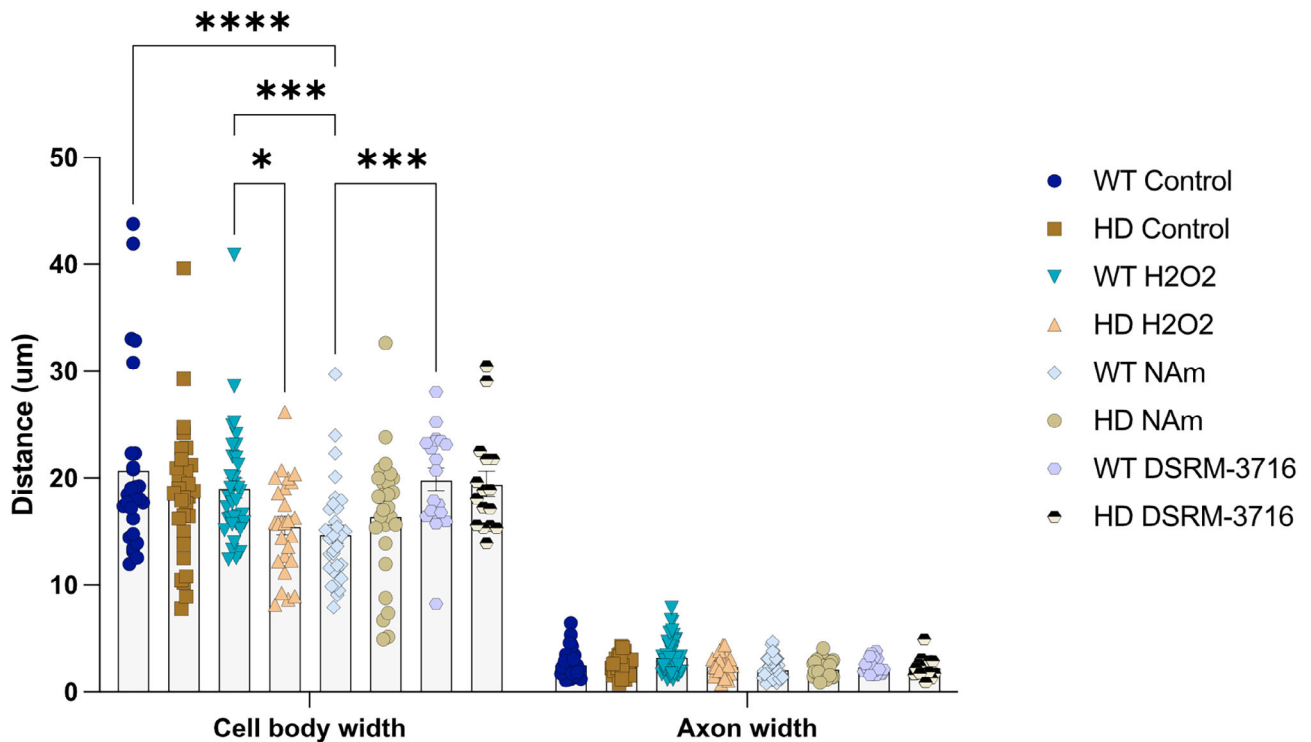


FIGURE 2 Legend on next page.

to be more resistant to NAM induced cell body shrinkage. We however did find a significant difference in the cell body widths of WT DRGs treated with H<sub>2</sub>O<sub>2</sub> and the cell body widths of HD DRGs treated with H<sub>2</sub>O<sub>2</sub>. HD DRGs treated with H<sub>2</sub>O<sub>2</sub> on average have smaller cell body widths, indicating that H<sub>2</sub>O<sub>2</sub> may have a shrinkage effect on HD cell bodies that WT DRGs are more resistant to. Finally, we found no difference in axon sizes between WT and HD models and across treatments. WT and HD cell bodies seem to be much more susceptible to treatment-induced shrinkage than DRG axons are.

### 3.2 | Axonal strength and neuronal resistance against laser cutting/slicing

Neuronal resistance against laser cutting was the second metric used to determine the differences in neuronal strength in WT and HD DRGs, and in their respective treatment groups. Figure 3A is a series of images of an HD Control DRG being cut eight times by the RoboLase system to fully cut through the axon. As the neuron is cut it forms *scar tissue* in a seemingly effective method to reduce damage from the laser (discussed below). When the laser hits the scar tissue, it forms a bubble that dissipates over time. The portion of the axon cut is enclosed within a white box in each image.

Figure 3B demonstrates the total time needed to cut through each DRG axon. The formation of scar tissue on the axon is accounted for in this figure as the total time measured included waiting for the bubble formed from slicing at scar tissue to shrink down enough so the cut site was once again visible. We found a significant difference in the time it took to cut through an untreated WT axon compared to the time that it took to cut through a wild-type axon treated with NAM. We found a similar difference between the time it took to cut through a WT

axon treated with H<sub>2</sub>O<sub>2</sub> compared to the time that it took to cut through a wild-type axon treated with NAM. Despite being shown to have a rescuing effect in other experiments [20], treatment with NAM reduced the total length of time needed to cut through wild-type DRGs, and therefore seems to reduce the axonal resistance against laser cutting. It, however, does not have the same effect on HD DRGs.

No difference was found between HD Control DRGs and HD DRGs treated with NAM. There is however a significant difference in the time it takes to cut through a WT axon treated with H<sub>2</sub>O<sub>2</sub> compared to the time that it takes to cut through an HD axon treated with H<sub>2</sub>O<sub>2</sub>. There is an additional significant difference in the time it takes to cut through an HD untreated (control) axon compared to the time that it takes to cut through an HD axon treated with H<sub>2</sub>O<sub>2</sub>. While H<sub>2</sub>O<sub>2</sub> treatment doesn't seem to have an effect on the resistance of WT neurons against axonal damage, treatment with H<sub>2</sub>O<sub>2</sub> reduces the total time to cut in HD neurons indicating that H<sub>2</sub>O<sub>2</sub> treatment reduces the axonal strength and in doing so reduces the ability of HD DRGs to resist damage.

Surprisingly, Figure 3B demonstrates that treatment with DSRM-3716 significantly reduces the time it takes to cut through the axon in both WT and HD DRGs. We found a significant difference between WT Control and WT DSRM-3716, between WT H<sub>2</sub>O<sub>2</sub> and WT DSRM-3716, and between HD Control and HD DSRM-3716. In all these cases, treatment with DSRM-3716 reduced the total time it took to cut through the axon.

Each data point in Figure 3C represents the total number of RoboLase system slices needed to fully cut through the axon of each DRG from each model. We found a significant difference in the number of laser slices needed to cut through an untreated WT axon compared to the number of laser slices needed to cut through a wild-type axon treated with NAM. We found this same

**FIGURE 2** (A) Representative image of cell body and axon width measurements for a WT Control dorsal root ganglion (DRG). (B) Representative image of cell body and axon widths measurements for an HD Control DRG. (C) Representative image of cell body and axon width measurements for a WT H<sub>2</sub>O<sub>2</sub> DRG. (D) Representative image of cell body and axon widths measurements for an HD H<sub>2</sub>O<sub>2</sub> DRG. (E) Representative image of cell body and axon width measurements for a WT NAM DRG. (F) Representative image of cell body and axon widths measurements for an HD NAM DRG. (G) Representative image of cell body and axon width measurements for a WT DSRM-3716 DRG. (H) Representative image of cell body and axon widths measurements for an HD DSRM-3716 DRG. (I) Bar graph demonstrating the differences in average cell body and axon width for WT and HD models and their respective treatments. Significant difference between WT Control and WT NAM cell body widths such that WT NAM DRGs on average have smaller cell body widths. \*\*\*\* $p < 0.0001$ . Significant difference between WT H<sub>2</sub>O<sub>2</sub> and WT NAM cell body widths such that WT NAM DRGs on average have smaller cell body widths. \*\*\* $p < 0.001$ . Significant difference between WT H<sub>2</sub>O<sub>2</sub> and HD H<sub>2</sub>O<sub>2</sub> cell body widths such that HD H<sub>2</sub>O<sub>2</sub> DRGs on average have smaller cell body widths. \* $p < 0.05$ . Significant difference between WT NAM and WT DSRM-3716 such that WT NAM DRGs on average have smaller cell body widths. \*\*\* $p < 0.001$  WT Control cell body  $n = 27$ ; HD Control cell body  $n = 31$ ; WT H<sub>2</sub>O<sub>2</sub> cell body  $n = 35$ ; HD H<sub>2</sub>O<sub>2</sub> cell body  $n = 26$ ; WT NAM cell body  $n = 31$ ; HD NAM cell body  $n = 27$ ; WT DSRM-3716 cell body  $n = 19$ ; HD DSRM-3716 cell body  $n = 16$ . WT Control axon  $n = 33$ ; HD Control axon  $n = 32$ ; WT H<sub>2</sub>O<sub>2</sub> axon  $n = 43$ ; HD H<sub>2</sub>O<sub>2</sub> axon  $n = 26$ ; WT NAM axon  $n = 42$ ; HD NAM axon  $n = 24$ ; WT DSRM-3716 axon  $n = 20$ ; HD DSRM-3716 axon  $n = 16$ .

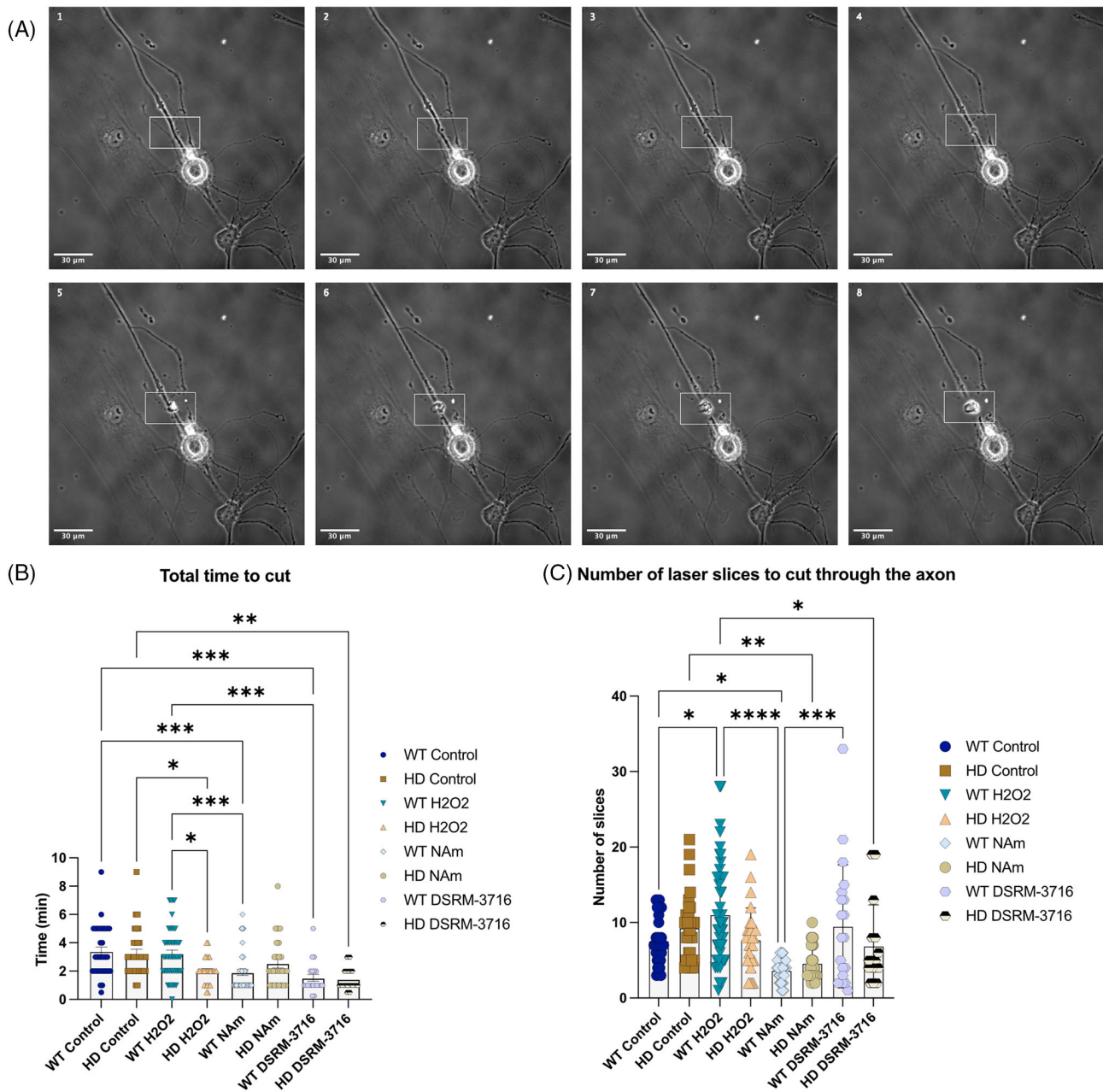


**FIGURE 3** (A) Robotic laser system slicing an HD Control dorsal root ganglion (DRG) eight times before the axon is fully severed. Scar tissue forms at the cut site making the axon more difficult to cut. The cut location in each image contained within the superimposed box. (B) Bar graph demonstrating the total time in minutes needed to fully cut through the DRG axon. Significant difference between WT Control and WT NAM such that WT NAM took much less time to cut through.  $***p < 0.001$ . Significant difference between WT H<sub>2</sub>O<sub>2</sub> and WT NAM such that WT NAM took less time to cut through.  $***p < 0.001$ . Significant difference between HD Control and HD H<sub>2</sub>O<sub>2</sub> such that HD H<sub>2</sub>O<sub>2</sub> took less time to cut through.  $*p < 0.05$ . Significant difference between WT H<sub>2</sub>O<sub>2</sub> and HD H<sub>2</sub>O<sub>2</sub> such that HD H<sub>2</sub>O<sub>2</sub> took less time to cut through.  $*p < 0.05$ . Significant difference between WT Control and WT DSRM-3716 such that WT DSRM-3716 took less time to cut through.  $***p < 0.001$ . Significant difference between HD Control and HD DSRM-3716 such that HD DSRM-3716 took less time to cut through.  $**p < 0.01$ . Significant difference between WT H<sub>2</sub>O<sub>2</sub> and WT DSRM-3716 such that WT DSRM-3716 took less time to cut through.  $***p < 0.001$ . WT Control  $n = 33$ ; HD Control  $n = 32$ ; WT H<sub>2</sub>O<sub>2</sub>  $n = 50$ ; HD H<sub>2</sub>O<sub>2</sub>  $n = 26$ ; WT NAM  $n = 43$ ; HD NAM  $n = 27$ ; WT DSRM-3716  $n = 20$ ; HD DSRM-3716  $n = 16$ . (C) Bar graph demonstrating the number of laser slices to cut through DRG axons in various models. Significant difference between WT Control and WT H<sub>2</sub>O<sub>2</sub> such that WT H<sub>2</sub>O<sub>2</sub> took more laser slices to cut through.  $*p < 0.05$ . Significant difference between WT Control and WT NAM such that WT NAM took fewer laser slices to cut through.  $*p < 0.05$ . Significant difference between HD Control and HD NAM such that HD NAM took fewer laser slices to cut through.  $**p < 0.01$ . Significant difference between WT H<sub>2</sub>O<sub>2</sub> and WT NAM such that WT NAM took much fewer laser slices to cut through.  $****p < 0.0001$ . Significant difference between WT H<sub>2</sub>O<sub>2</sub> and WT DSRM-3716 such that WT NAM took much fewer laser slices to cut through.  $***p < 0.001$ . WT Control  $n = 33$ ; HD Control  $n = 32$ ; WT H<sub>2</sub>O<sub>2</sub>  $n = 50$ ; HD H<sub>2</sub>O<sub>2</sub>  $n = 26$ ; WT NAM  $n = 43$ ; HD NAM  $n = 27$ ; WT DSRM-3716  $n = 20$ ; HD DSRM-3716  $n = 16$ .



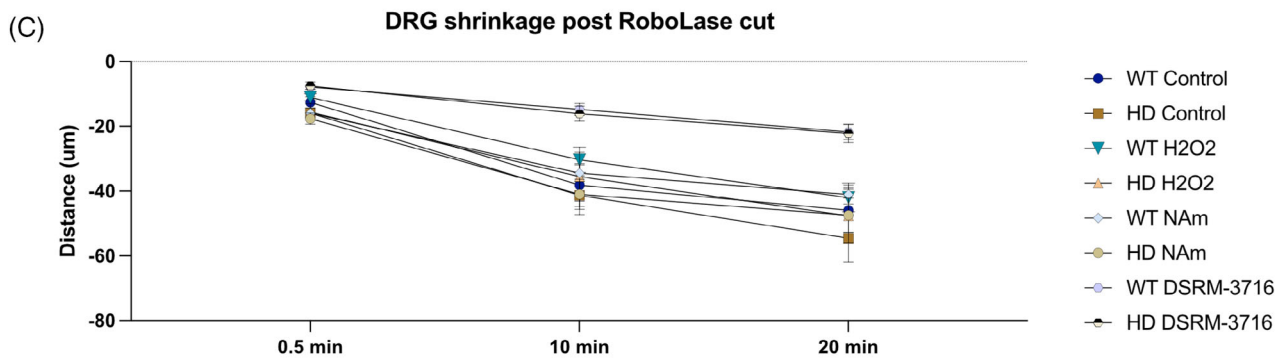
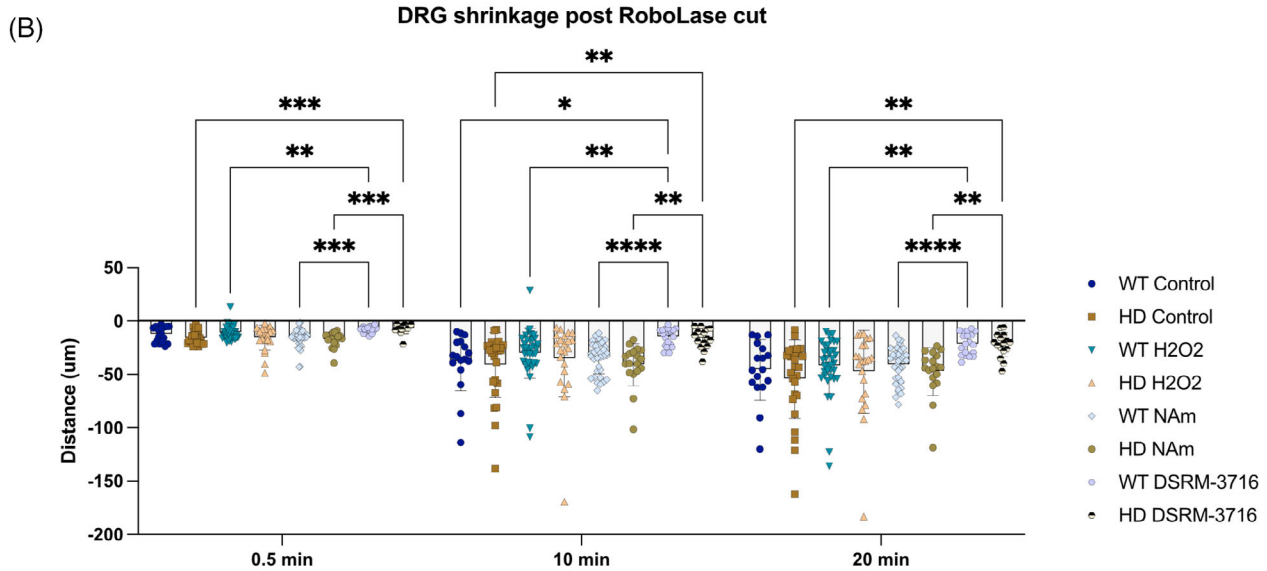
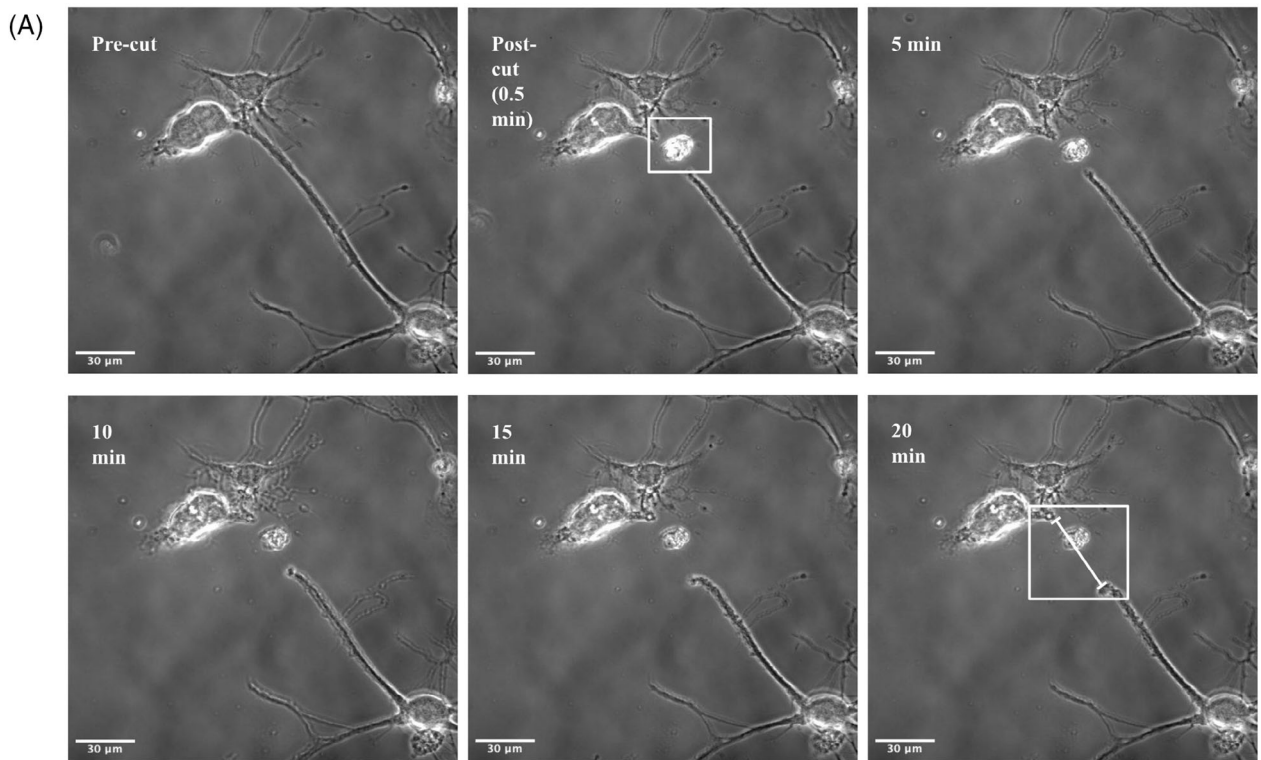


FIGURE 4 Legend on next page.

difference when comparing WT DRGs treated with NAM to WT DRGs treated with H<sub>2</sub>O<sub>2</sub> and also to WT DRGs treated with DSRM-3716. NAM reduces the total number of laser slices needed to cut through WT DRGs, which supports the results from Figure 3B. Figure 3C demonstrates similar effects of NAM treatment on HD DRGs. Treatment with NAM significantly reduces the number of laser slices needed to fully cut through the axon, indicating that NAM might also reduce axonal strength and neuronal resistance against laser cutting in HD DRGs. Finally, Figure 3C demonstrates that it takes significantly more laser cuts to cut through WT H<sub>2</sub>O<sub>2</sub> DRGs compared to WT Control DRGs. WT H<sub>2</sub>O<sub>2</sub> DRGs seem to have increased axonal resistance against neuronal damage compared to WT Control DRGs.

### 3.3 | DRG shrinkage post-RoboLase cut

Finally, we wanted to determine if Huntington's disease, oxidative stress, nicotinamide, or SARM1 inhibition had any effect on axonal shrinkage post-RoboLase cut. Figure 4A shows a series of images of an HD Control DRG before being cut by the RoboLase system (pre-cut), after 13 slices from the RoboLase system (post-cut), 5 min post-cut, 10 min post-cut, 15 min post-cut, and 20 min post-cut. The images clearly show the axon shrinking after being cut by the laser. The images also clearly show the scar tissue that builds up as a result of the laser damage. This scar tissue is boxed in white in the post-cut image.

To calculate the amount of shrinkage the distance from one cut end to the other cut end was measured. An example of this measurement is shown in the 20 min post-cut image of Figure 4A. Figure 4B,C demonstrates two different visualizations of the axonal shrinkage data at three different time intervals: immediately post RoboLase system cut (0.5 min), 10 min after RoboLase system

cut, and 20 min after RoboLase system cut. Figure 4B represents the data in bar graph style with the individual values for each DRG superimposed on top of the bar graph. Figure 4B also clearly shows the high levels of variation in shrinkage within each model. Shrinkage variation was especially high in the HD Control model. Figure 4C represents data in summary form with superimposed symbols demonstrating the average shrinkage for each model post-cut (0.5 min), at 10 min post-cut, and at 20 min post-cut. Figure 4C demonstrates that HD models may shrink slightly more than WT models, but this difference is non-significant. Additionally, comparisons between WT and HD Control and respective H<sub>2</sub>O<sub>2</sub> and NAM treatment groups in Figure 4B,C were also non-significant. However, we did find significant differences in shrinkage patterns of DRGs treated with DSRM-3716.

WT DRGs treated with DSRM-3716 demonstrated decreased shrinkage at 0.5 min post-cut, 10 min post-cut, and 20 min post-cut compared to WT DRGs treated with NAM and WT DRGs treated with H<sub>2</sub>O<sub>2</sub>. At 10 min post-cut, WT DRGs treated with DSRM-3716 demonstrated decreased shrinkage compared to WT Control DRGs as well. HD DRGs treated with DSRM-3716 demonstrated decreased shrinkage at 0.5 min post-cut, 10 min post-cut, and 20 min post-cut compared to HD Control DRGs and HD DRGs treated with NAM.

## 4 | DISCUSSION

Previous studies on Huntington's disease patients and transgenic mice have found that mHTT accumulates in the nuclei and processes of the neuron [37–40]. The accumulation of mHTT proteins in the cell body could provide an explanation for why the wild-type DRG cell bodies substantially shrank in response to NAM while Huntington's disease DRG cell bodies did not change in response to NAM treatment (Figure 2I). Upon treatment

**FIGURE 4** (A) Images of an HD Control dorsal root ganglion (DRG) before slicing from the RoboLase system (pre-cut), after 13 slices from the RoboLase system (post-cut), 5 min post-cut, 10 min post-cut, 15 min post-cut, and 20 min post-cut. (B) Bar graph representing the amount of shrinkage of each model post-cut (0.5 min), 10 min post-cut, and 20 min post-cut. High variation within Control, H<sub>2</sub>O<sub>2</sub>, and NAM models. Significant difference between WT H<sub>2</sub>O<sub>2</sub> and WT DSRM-3716 such that WT DSRM-3716 demonstrated less shrinkage at all time points. \*\* $p < 0.01$ . Significant difference between WT NAM and WT DSRM-3716 such that WT DSRM-3716 demonstrated less shrinkage at all time points. \*\*\* $p < 0.001$  at 0.5 min, \*\*\*\* $p < 0.0001$  at 10 min and 20 min. Significant difference between WT Control and WT DSRM-3716 at 10 min such that WT DSRM-3716 demonstrated less shrinkage. \* $p < 0.05$ . Significant difference between HD Control and HD DSRM-3716 such that HD DSRM-3716 demonstrated less shrinkage at all time points. \*\*\* $p < 0.001$  at 0.5 min, \*\* $p < 0.01$  at 10 min and 20 min. Significant difference between HD NAM and HD DSRM-3716 such that HD DSRM-3716 demonstrated less shrinkage at all time points. \*\*\* $p < 0.001$  at 0.5 min, \*\* $p < 0.01$  at 10 min and 20 min. (C) Superimposed symbols graph representing the amount of shrinkage of each model post-cut (0.5 min), 10 min post-cut, and 20 min post-cut. Bars represent the standard error of the mean for each model. WT Control  $n = 17$ ; HD Control  $n = 26$ ; WT H<sub>2</sub>O<sub>2</sub>  $n = 36$ ; HD H<sub>2</sub>O<sub>2</sub>  $n = 22$ ; WT NAM  $n = 34$ ; HD NAM  $n = 18$ ; WT DSRM-3716  $n = 20$ ; HD DSRM-3716  $n = 16$ .

with  $H_2O_2$ , a difference in cell body size was seen between wild-type and Huntington's disease DRGs, with Huntington's disease DRGs having slightly smaller cell bodies (Figure 2I). We can conclude that wild-type DRGs are more susceptible to NAM-induced morphology changes than oxidative stress-induced morphology changes. Additionally, despite the accumulation of mHTT proteins, Huntington's disease DRGs do seem to be somewhat susceptible to oxidative stress-induced morphology changes. In contrast, neither wild-type nor Huntington's disease DRGs demonstrated any cell body shrinkage when exposed to SARM1 inhibitor DSRM-3716. Cell shrinkage is linked to programmed cell death signals [41]. We can conclude that both NAM and  $H_2O_2$  have cytotoxic effects on wild type and HD neurons, respectively. We can further conclude that DSRM-3716 does not have cytotoxic effects on wild type or HD neurons.

However, while NAM and  $H_2O_2$  had demonstrated effects on wild-type and Huntington's disease DRG cell body widths, they did not have any effect on axonal widths (Figure 2I). We hypothesize that this is because axons are full of cytoskeleton, microtubules, actins, and neurofilaments, whereas cell bodies are more fluid [42]. The additional stability of the axon may confer resistance to drug-induced morphology changes, resulting in NAM and  $H_2O_2$  treatments having no effect on the DRG axon widths despite having a significant effect on the cell body widths.

Huntington's disease is classified as a CNS disease with its effects mainly resulting in the degeneration of the striatum and the thinning of the cortical ribbon [7–12, 43, 44]. However, our studies on the morphological differences between wild-type and Huntington's disease DRGs, and their treatment groups, indicate that wild-type and Huntington's disease neurons have different reactions to different treatments despite the classification of DRGs as PNS neurons. Our axonal strength studies demonstrated in Figure 3 further support the conclusion that Huntington's disease significantly impacts the PNS. Figure 3B demonstrates similar results to those in Figure 2I, with NAM treatment detrimentally affecting the neuron by decreasing axonal strength in wild-type DRGs. Figure 3C demonstrates an additional significant difference between the axonal strength of untreated wild-type DRGs and wild-type DRGs exposed to  $H_2O_2$ . In this experiment, we found that wild-type DRG axons treated with  $H_2O_2$  were more resistant to damage than wild-type untreated axons, in the sense that it took many more laser slices to cut through the  $H_2O_2$  treated wild-type DRG compared to WT Control axons. A similar increase in axonal resistance against damage was not found in Huntington's disease DRGs. Interestingly, we also did not find a difference in the time it takes to cut through the  $H_2O_2$  treated axons, compared to the control (Figure 3B).

Oxidative stress has been found to dramatically increase microtubule networks inside cardiac myocytes [45]. Since scar tissue plays a large role in increasing the total time to cut, our results indicate that in wild-type DRGs,  $H_2O_2$  may have a strengthening effect on the microtubule networks, resulting in an increase in the number of slices needed to cut through the neuron, while simultaneously having a preventative effect on the development and strength of scar tissue, resulting in the non-significant difference in total time until cut through. Treatment with  $H_2O_2$  on Huntington's disease DRGs was found to reduce the total time to cut through the axon while having no significant effect on the number of laser slices to cut through the axon (Figure 3B,C). These results indicate that  $H_2O_2$  may have a preventative effect on the development and strength of scar tissue in Huntington's disease DRGs but doesn't seem to significantly impact microtubular networks.

Similar to  $H_2O_2$  treatment, treatment with DSRM-3716 significantly reduced the amount of time it took to cut through both wild-type and Huntington's disease DRG axons (Figure 3B). However, treatment with DSRM-3716 did not reduce the number of laser slices to cut through the axon for either model (Figure 3C). These results indicate that DSRM-3716 may too have a preventative effect on the development and strength of scar tissue in wild-type and Huntington's disease DRGs.

Despite the effect of DSRM-3716 on axonal strength against damage shown in Figure 3, treatment DSRM-3716 did reduce degeneration in both wild-type and Huntington's disease DRGs (Figure 4B,C). This reduction in degeneration was seen at each time point: immediately post-cut (0.5 min), 10 min post-cut, and 20 min post-cut. These results support the longstanding determination that SARM1 inhibition results in protection from neuronal degeneration [31].

As mentioned above, NAM has conflictingly been described as having a neuroprotective effect, and as having no effect [28, 29]. Our results indicate that NAM treatment both induced cell body shrinkage in wild-type DRGs and reduced axonal strength against laser-induced damage (Figures 2 and 3). This result was highly unexpected and is indicative that despite its rescuing effects, high concentrations NAM can be neurotoxic.

One question we plan to address in future experiments is if the use of embryonic and P0 DRGs played a role in our shrinkage results, especially given the high amount of variability of the embryonic and P0 DRG shrinkage patterns seen in Figure 4B,C. Since Huntington's disease onset is generally mid to late in life, these future studies will focus on determining if older DRGs demonstrate differences in shrinkage patterns. Given that our use of a NAM concentration of 24.5 mM was in the range of safe concentrations, yet still proved to be

neurotoxic, future studies will also work to determine the specific NAM concentration that the neuroprotective effects become neurotoxic in DRGs. In the future, we hope to create a new metric of safe NAM concentrations in DRGs.

### AUTHOR CONTRIBUTIONS

S.B. wrote the first draft of the manuscript. S.B., A.W., J.Y., and L.S. performed the experiments. S.B., S.C., J.Y., and A.W. performed quantifications and statistical analysis. L.S., V.G., S.B., J.Y., and A.W. set up the RoboLase laser and monitored axonal shrinkage. V.G. designed the experiment. S.B., A.S., S.S.C., and C.W. performed breeding, dissections, monitored, and maintained cells. All authors contributed to manuscript revision, read, and approved the submitted version.

### FUNDING INFORMATION

The material presented in this manuscript was supported by a gift from the Beckman Laser Institute Inc.

### CONFLICT OF INTEREST STATEMENT

The authors declare no conflict of interest.

### DATA AVAILABILITY STATEMENT

The authentic contributions presented in this study are included in the article and further inquiries can be directed to the corresponding authors.

### ORCID

Linda Shi  <https://orcid.org/0009-0004-8602-2813>

### REFERENCES

- [1] S. Davies, D. B. Ramsden, *Mol. Pathol.* **2001**, *54*, 409.
- [2] Group, T.H.s.D.C.R, *Cell* **1993**, *72*, 971.
- [3] L. Mangiarini, K. Sathasivam, M. Seller, B. Cozens, A. Harper, C. Hetherington, M. Lawton, Y. Trottier, H. Lehrach, S. W. Davies, G. P. Bates, *Cell* **1996**, *87*, 493.
- [4] A. H. Sharp, S. J. Loev, G. Schilling, S. H. Li, X. J. Li, J. Bao, M. V. Wagster, J. A. Kotzuk, J. P. Steiner, A. Lo, J. Hedreen, S. Sisodia, S. H. Snyder, T. M. Dawson, D. K. Ryugo, C. A. Ross, *Neuron* **1995**, *14*, 1065.
- [5] R. Ghosh, S. J. Tabrizi, *Adv. Exp. Med. Biol.* **2018**, *1049*, 1.
- [6] S. J. Tabrizi, B. R. Leavitt, G. B. Landwehrmeyer, E. J. Wild, C. Saft, R. A. Barker, N. F. Blair, D. Craufurd, J. Priller, H. Rickards, A. Rosser, H. B. Kordasiewicz, C. Czech, E. E. Swayze, D. A. Norris, T. Baumann, I. Gerlach, S. A. Schobel, E. Paz, et al., *N. Engl. J. Med.* **2019**, *380*, 2307.
- [7] A. Reiner, R. L. Albin, K. D. Anderson, C. J. D'Amato, J. B. Penney, A. B. Young, *Proc. Natl. Acad. Sci. U. S. A.* **1988**, *85*, 5733.
- [8] R. L. Albin, A. Reiner, K. D. Anderson, J. B. Penney, A. B. Young, *Ann. Neurol.* **1990**, *27*, 357.
- [9] R. L. Albin, A. Reiner, K. D. Anderson, L. S. Dure 4th, B. Handelin, R. Balfour, W. O. Whetsell Jr., J. B. Penney, A. B. Young, *Ann. Neurol.* **1992**, *31*, 425.
- [10] R. L. Albin, *Ann. Neurol.* **1995**, *38*, 835.
- [11] A. Reiner, E. Shelby, H. Wang, Z. Demarch, Y. Deng, N. H. Guley, V. Hogg, R. Roxburgh, L. J. Tippett, H. J. Waldvogel, R. L. Faull, *Mov. Disord.* **2013**, *28*, 1691.
- [12] H. D. Rosas, A. K. Liu, S. Hersch, M. Glessner, R. J. Ferrante, D. H. Salat, A. van der Kouwe, B. G. Jenkins, A. M. Dale, B. Fischl, *Neurology* **2002**, *58*, 695.
- [13] I. Han, Y. You, J. H. Kordower, S. T. Brady, G. A. Morfini, *J. Neurochem.* **2010**, *113*, 1073.
- [14] G. P. Bates, R. Dorsey, J. F. Gusella, M. R. Hayden, C. Kay, B. R. Leavitt, M. Nance, C. A. Ross, R. I. Scahill, R. Wetzell, E. J. Wild, S. J. Tabrizi, *Dis. Primers* **2015**, *1*, 15005.
- [15] N. G. Rojas, M. E. Cesarini, G. Peker, G. A. da Prat, J. L. Etcheverry, E. M. Gatto, *J. Neurol. Res.* **2022**, *12*, 93.
- [16] J. S. Paulsen, D. R. Langbehn, J. C. Stout, E. Aylward, C. A. Ross, M. Nance, M. Guttman, S. Johnson, M. MacDonald, L. J. Beglinger, K. Duff, E. Kayson, K. Biglan, I. Shoulson, D. Oakes, M. Hayden, *J. Neurol. Neurosurg. Psychiatry* **2008**, *79*, 874.
- [17] E. van Duijn, E. M. Kingma, R. C. van der Mast, *J. Neuropsychiatry Clin. Neurosci.* **2007**, *19*, 441.
- [18] Craufurd, D., & Snowden, J. S. Neuropsychiatry and Neuropsychology. in *Huntington's Disease*, Oxford University Press, Oxford **2014**. <https://doi.org/10.1093/MED/9780199929146.003.0003>
- [19] S. J. Tabrizi, R. I. Scahill, G. Owen, A. Durr, B. R. Leavitt, R. A. Roos, B. Borowsky, B. Landwehrmeyer, C. Frost, H. Johnson, D. Craufurd, R. Reilmann, J. C. Stout, D. R. Langbehn, *Lancet Neurol.* **2013**, *12*, 637.
- [20] E. A. Epping, J. I. Kim, D. Craufurd, T. M. Brashers-Krug, K. E. Anderson, E. McCusker, J. Luther, J. D. Long, J. S. Paulsen, *Am. J. Psychiatr.* **2016**, *173*, 187.
- [21] N. P. Rocha, B. Mwangi, C. A. G. Candano, C. Sampaio, E. F. Stimming, A. L. Teixeira, *Front. Neurol.* **2018**, *9*, 415113.
- [22] J. S. Paulsen, K. F. Hoth, C. Nehl, L. Stierman, *Am. J. Psychiatry* **2005**, *162*, 725.
- [23] C. L. Chuang, F. Demontis, *Ageing Res. Rev.* **2021**, *69*, 101358.
- [24] Y. J. Song, F. E. Jensen, D. M. Talos, *Neuronal Chloride Transporters in Health and Disease*, Academic Press, Cambridge, MA **2020**, p. 215. <https://doi.org/10.1016/B978-0-12-815318-5.00010-8>
- [25] N. Ahimsadason, V. Reddy, M. Z. Khan Suheb, A. Kumar, *StatPearls [Internet]*. StatPearls Publishing, Florida **2023**. <https://www.ncbi.nlm.nih.gov/books/NBK532291/>
- [26] K. R. Hoyt, A. J. Gallagher, T. G. Hastings, I. J. Reynolds, *Neurochem. Res.* **1997**, *22*, 333.
- [27] C. Fang, D. Bourdette, G. Banker, *Mol. Neurodegener.* **2012**, *7*, 29.
- [28] J. Wang, Z. He, *Cell Adhes. Migr.* **2009**, *3*, 77.
- [29] P. H. Y. S. I. O. Lo, M. V. Damgaard, J. T. Treebak, *Sci. Adv.* **2023**, *9*. <https://doi.org/10.1126/SCIADV.ADI4862>
- [30] J. Y. Kim, H. Lee, J. Woo, W. Yue, K. Kim, S. Choi, J. J. Jang, Y. Kim, I. A. Park, D. Han, H. S. Ryu, *Sci. Rep.* **2017**, *7*, 3466.
- [31] H. S. Loring, P. R. Thompson, *Cell Chem. Biol.* **2020**, *27*, 1.
- [32] M. Gray, D. I. Shirasaki, C. Cepeda, V. M. André, B. Wilburn, X. H. Lu, J. Tao, I. Yamazaki, S. H. Li, Y. E. Sun, X. J. Li, M. S. Levine, X. W. Yang, *J. Neurosci. Off. J. Soc. Neurosci.* **2008**, *28*, 6182.
- [33] J. N. Sleight, G. A. Weir, G. Schiavo, *BMC. Res. Notes* **2015**, *9*, 82.



- [34] T. Heinrich, C. A. Hübner, I. Kurth, *Bio-Protoc.* **2016**, 6, e1785.
- [35] J. Wang, Q. Zhai, Y. Chen, E. Lin, W. Gu, M. W. McBurney, Z. He, *J. Cell Biol.* **2005**, 170, 349.
- [36] R. O. Hughes, T. Bosanac, X. Mao, T. M. Engber, A. DiAntonio, J. Milbrandt, R. Devraj, R. Krauss, *Cell Rep.* **2021**, 34, 108588.
- [37] M. DiFiglia, E. Sapp, K. O. Chase, S. W. Davies, G. P. Bates, J. P. Vonsattel, N. Aronin, *Science* **1997**, 277, 1990.
- [38] S. W. Davies, M. Turmaine, B. A. Cozens, M. DiFiglia, A. H. Sharp, C. A. Ross, E. Scherzinger, E. E. Wanker, L. Mangiarini, G. P. Bates, *Cell* **1997**, 90, 537.
- [39] H. Li, S. H. Li, A. L. Cheng, L. Mangiarini, G. P. Bates, X. J. Li, *Hum. Mol. Genet.* **1999**, 8, 1227.
- [40] G. Schilling, M. W. Becher, A. H. Sharp, H. A. Jinnah, K. Duan, J. A. Kotzuk, H. H. Slunt, T. Ratovitski, J. K. Cooper, N. A. Jenkins, N. G. Copeland, D. L. Price, C. A. Ross, D. R. Borchelt, *Hum. Mol. Genet.* **1999**, 8, 397.
- [41] M. Song, S. P. Yu, *Transl. Stroke Res.* **2014**, 5, 17.
- [42] E. L. Holzbaur, S. S. Scherer, *N. Engl. J. Med.* **2011**, 365, 2330.
- [43] R. Morigaki, S. Goto, *Brain Sci.* **2017**, 7, 2.
- [44] E. M. Gatto, N. G. Rojas, G. Persi, J. L. Etcheverry, M. E. Cesarini, C. Perandones, *Clin. Parkinsonism Relat. Disord.* **2020**, 3, 100056.
- [45] R. R. Goldblum, M. McClellan, K. White, S. J. Gonzalez, B. R. Thompson, H. X. Vang, H. Cohen, L. A. Higgins, T. W. Markowski, T. Y. Yang, J. M. Metzger, M. K. Gardner, *Dev. Cell* **2021**, 56, 2252.

## AUTHOR BIOGRAPHIES

**Sophia Barber** is a recent University of California San Diego (UCSD) magna cum laude graduate and Goldwater Scholar with a B.S. in Neurobiology. In 2021 Sophia joined the Wu Lab at UCSD where she studied treatments for chemotherapy induced peripheral neuropathy and tracked lysosomal and mitochondrial size and speed across various disease models. She then began collaborating with the Berns Lab where she studied the effects of oxidative stress, nicotinamide, and SARM1 inhibition on Huntington's disease dorsal root ganglions (DRGs). Sophia is currently working with Dr. T.J. Seago at the University of Florida developing user interfaces that support computational modeling in research and education. Sophia has published three journal papers and 29 conference papers/posters in the past 3 years. She hopes to become a physician-scientist and will be applying to medical school with her fiancé in the 2024 medical school application cycle.

**Dr. Veronica Gomez-Godinez** is a project scientist at the University of California-San Diego working in the Cellular Biophotonics Laboratory where she utilizes lasers to probe single cells and structures within cells. Dr. Gomez-Godinez is also a chief scientist for the OPALS summer internship program where she

mentors students on research projects related to calcium signaling during neurodegeneration. She has made contributions to the field of DNA repair by being one of the first to demonstrate that mitotic cells are capable of initiating DNA synthesis in response to damage. Additionally, she has contributed to our understanding of astrocytic responses to cell injury where she demonstrated that a single cell death can lead to interruptions in cells spontaneous activity.

**Joy Young** is currently a student at the University of California, Berkeley, studying Chemical Biology. She graduated from Camas High School in 2023. She conducted research under Dr. Linda Shi from 2021 to 2023 at the Biophotonics Technology Center at the University of California, San Diego. The research focused on the effectiveness of Mdiv-1 on neurons with Charcot Marie Tooth Type 2B Disease and the effects of hydrogen peroxide on neurons with Huntington's Disease. She presented the research through posters at the virtual 2021 American Society for Cell Biology Conference and at the 2022 Biomedical Engineering Society Conference. She was also second author for a poster presented at the 2022 International Society for Optics and Photonics (SPIE) Conference.

**Abigail Wei** is a driven scientist in her freshman year at the University of California, Riverside, where she is pursuing a Bachelor of Science in Biology with a focus on pre-medicine. Over the past 4 years, starting in 2020, Abigail has been actively involved in research, working under the guidance of Dr. Linda Shi at the University of California, San Diego. She has three published research papers in the realm of combining biophotonics and neuroscience, where she used—and is skilled in—both Image-J and Matlab to collect and analyze more than a hundred cells. In 2023, Abigail currently holds the position of a Research Assistant at Dr. Edward Korzus' Lab within the Department of Neuroscience and Psychology at the University of California, Riverside. Her current research focus revolves around understanding the distinction of fear in relation to learning and behavior specifically the interaction between the hippocampus and the pre-frontal cortex. Furthermore, Abigail Wei has been committed as the founder of Bridge-Mexico Missions, since 2019. Going to Ensenada, Mexico twice a year, her organization provides medical services in the areas of optometry, dentistry, physical therapy, and basic healthcare to underserved communities. Aside from academics, Abigail Wei enjoys reading, ceramic painting, hiking, and swimming.

**Sarah Chen** is a high school sophomore at Pacific Ridge School (PRS) in Carlsbad, California. In mid-2023, Sarah established a Biomedical Engineering Society (BMES) student chapter at her school, where she currently holds the position of President. In this chapter, Sarah has been actively involved with planning lab visits, inviting speakers, meeting with other chapters in the area, and collaborating with fellow members to teach middle schoolers about STEM. Since 2022, Sarah has continually participated in research under the guidance of Dr. Linda Shi at the University of California, San Diego. She has analyzed hundreds of cells, using Image J, a process she is skilled in and has taught to many other students. During the UCSD 2023 summer Outreach Program for Advanced Learning in STEM, Sarah furthered her work on axon degeneration of neurodegenerative diseases using laser ablation. Following her research, Sarah has published two posters and is an author of one research paper. At her high school, Sarah actively participates in numerous clubs, including SWENext (Society of Woman Engineers), robotics, and student council, where she has held leadership positions for over 5 years and is currently class representative. She has been on the PRS varsity dance team for 2 years and has danced for over 10 years. Sarah's other hobbies include crocheting and photography.

**Anna Snissarenko** is a third-year undergraduate student-athlete on the women's tennis team at University of California, San Diego (UCSD). She currently holds an IGETC degree from Antelope Valley College and is pursuing a Bachelor of Science in Human Biology at UCSD. Since March 2022, Anna has been actively involved in research as a lab assistant at the Dr. Wu neuroscience lab at the UCSD School of Medicine. Her research focuses on investigating mitochondria dysfunction in neurodegenerative diseases, such as Huntington's disease and Alzheimer's disease. Anna is on the pre-med track and is aspiring to become a physician one day. She has been actively immersing herself in the medical field by graduating from the Kaiser Permanente Medical Explorers program, shadowing doctors at the Antelope Valley Medical Center, attending the annual Southern California Permanente Medical Group (SCPMG) Women in Medicine Symposium, and volunteering at the local Kaiser Permanente clinic. Most notably, Anna was a part of the medical mission trip hosted by Loma Linda University to Ishaka, Uganda in June 2023, where more than 8800 patients were treated at the free medical clinic.

**Sze Sze** is currently a third year undergraduate student at UC San Diego majoring in human biology. She is a neurodegenerative disease lab assistant in Alzheimer's disease, Parkinson's disease and Huntington's disease. She has also worked as an intern at Food Angel and Hong Kong Applied Science and Technology Research Institute in Hong Kong and mentored a high school lab research internship. She has also served as a hospice volunteer at a UCSD affiliated elderly home.

**Dr. Chengbiao Wu** is an Associate Professor in the Department of Neurosciences, University of California San Diego (UCSD). Dr. Wu received his PhD from Queen's University, Canada and then trained at NIH, UT Southwestern Medical Center at Dallas and Stanford University. He joined UCSD Neurosciences faculty in 2009. At UCSD, Dr. Wu's research focuses on the investigation of the cellular and molecular mechanisms of disorders in both the Central Nervous System (CNS) and the Peripheral Nervous System (PNS). Using mouse models of Alzheimer's, Huntington's and Parkinson's disease, his study has uncovered that axonal dysfunction and deficient axonal transport of neurotrophic factors and signaling is an early signature of cellular pathogenic manifestations in neurodegeneration. Dr. Wu's research has also made significant contribution to our understanding of peripheral sensory neuropathy such as Charcot Marie Tooth 2B (CMT2B) and hereditary autonomic sensory neuropathy V diseases. And more importantly, his recent study has established that a missense mutation in nerve growth factor (NGF) decouples the neurotrophic function from the pain causing effect associated with normal NGF, a road blockade that has long prevented the use of NGF for treating many human conditions such as diabetic neuropathy and HIV-, chemotherapy-induced neuropathy. Dr. Wu is the author of over 60 publications including *Journal of Clinical Investigation (JCI)*, *Proceedings of the National Academy of Sciences (PNAS)*, *Journal of Neuroscience and Progress in Neurobiology*, and so forth.

**Dr. Linda Shi** is the PI at Biophotonics Lab and Co-director of Biophotonics Technology Center at UCSD Institute of Engineering in Medicine(IEM). She is also the director for IEM OPALS internship program. Dr. Shi has worked in Biophotonics Lab at UCSD since 2004 with a background in Electrical and Mechanical Engineering. She designed the laser trapping and laser ablation system (robolase) to investigate the heart cell repair after physiological damage, the flagellar length equalization, measure calcium signal changes on the retinal ganglion cells with

glaucomatous, study the ultrafast dynamics of molecular vibrational polaritons, and hold and manipulate microbes to measure the effect on enteroendocrine cells in the gastrointestinal. Dr. Shi published 53 journal papers and 49 conference papers/posters in the past 20 years.

**How to cite this article:** S. Barber, V. Gomez-Godinez, J. Young, A. Wei, S. Chen, A. Snissarenko, S. S. Chan, C. Wu, L. Shi, *J. Biophotonics* **2024**, e202300370. <https://doi.org/10.1002/jbio.202300370>